

AN INTERVAL BRANCH AND BOUND PROCEDURE TO COMPUTE LIMIT CYCLES IN UNCERTAIN NONLINEAR SYSTEMS

P. S. V. NATARAJ AND J. J. BARVE

*Systems and Control Engineering Group
Department of Electrical Engineering
Indian Institute of Technology, Bombay, India 400 076
Email: nataraj@ee.iitb.ernet.in*

ABSTRACT. An interval analysis based branch and bound procedure is presented for limit cycle analysis of uncertain nonlinear systems using the describing function approach. The procedure can be applied to a very wide class of uncertain linear and nonlinear elements having general nonlinear parametric uncertainty structures. The procedure is demonstrated on some difficult examples.

Keywords: Describing Functions, Interval Analysis, Limit Cycles, Nonlinear Control, Uncertain Systems.

Glossary

DF: Describing function

LTI: Linear time invariant

Notation

Boldface: Interval quantities

a : Amplitude of periodic input signal to nonlinear element

Box: An n -dimensional parallelepiped having sides parallel to the coordinate axes.

$f^{\text{range}}(\mathbf{x})$: The range of an arbitrary function f over a box \mathbf{x} , i.e., $f^{\text{range}}(\mathbf{x}) := \{f(x) : x \in \mathbf{x}\}$

$\mathbf{f}(\mathbf{x})$: A natural interval extension of function f on box \mathbf{x} .

$\mathbf{f}'(\mathbf{x})$: A natural interval extension of Jacobian of function f on box \mathbf{x} .

$\mathbf{f}'_x(\mathbf{x})$: A natural interval extension of Jacobian of function f w.r.t. x on box \mathbf{x} .

$\mathbf{K}(\mathbf{x}, \mathbf{p})$: The generalized Krawczyk operator

\mathbf{p} : Box of (uncertain) parameters of nonlinear system

\mathbf{x} : Box of amplitude and frequency ranges (such a box is a trial region for finding limit cycle points)

x^* : A limit cycle point, i.e., amplitude and frequency of the predicted limit cycle

\hat{x} : Midpoint of box \mathbf{x}

ω : Frequency of periodic input signal to nonlinear element

1. INTRODUCTION

The popular describing function (DF) analysis is mainly employed to predict the existence of constant amplitude oscillations in closed loop nonlinear systems, known as *limit cycles*. If limit cycles are predicted, then it is also of interest to know the number of limit cycles along with their frequencies, amplitudes and characteristics such as stability or instability. DF analysis occasionally fails, particularly when the system under consideration does not satisfy the assumption of the ‘filtering hypothesis’ [7]. It is also possible for DF analysis to predict no limit cycles, even when a limit cycle actually exists. Despite these limitations, DF analysis has been successfully used in many practical applications, for example, see [2], [4], [18]. For a comprehensive treatment of the DF approach, see [7], [3].

In real life, often there are uncertainties in the parameters of the nonlinear system. The DF approach to analysis of uncertain nonlinear systems has only recently attracted the attention of researchers. Fadali and Chachavalvoong [5] overbound the unknown coefficients of the system characteristic equation and use

Kharitonov's theorem to do the overall stability test, but unless the numerator of the LTI element is constant, the method gives conservative results. Tierno [21] fits a rational approximation to the DF of the nonlinear element, and incorporates DF analysis into a generalized structured singular value (μ) framework of robustness analysis. However, his method can be used only when a good rational approximation to the DF is obtainable. Ferreres and Fromion [6] propose a μ based method for limit cycle analysis, but their method is limited to uncertainties in the LTI element. Impram and Munro [9] pose the DF analysis problem in a generalized interval polynomial framework, but their method is conservative unless the coefficients of the LTI element have interval or affine linear uncertainty structure. Moreover, the aforementioned methods are restricted to LTI elements represented by *rational* transfer functions.

In this paper, we present a procedure for limit cycle analysis of nonlinear systems with separable nonlinearities, in the presence of parametric uncertainties in the LTI and nonlinear elements shown in Fig. 2.1. We formulate the problem of finding the limit cycle points as one of finding zeros of a parameter-dependent system of nonlinear equations. We then apply tools of interval analysis (IA) [14] in the form of a procedure for solving the zero finding problem. IA has proven itself useful in many contexts, and has been particularly successful in branch and bound procedures for finding all zeros of a system of nonlinear equations. Interval branch and bound procedures for finding all zeros use a combination of a computational existence procedure and a tessellation (i.e., generalized bisection) process. In our procedure, we use the generalized Krawczyk method to computationally verify the existence or non-existence of a zero in a given region. The generalized Krawczyk method is powerful as a computational fixed point theorem, and has a clear relationship to the well-known Brouwer fixed point theorem [11]. Moreover, the generalized Krawczyk method also possesses a computationally verifiable sufficient condition for guaranteed convergence to all the zeros in a given region, and further, this convergence can be obtained in a *finite* number of steps if we use rounded interval arithmetic on a computing machine.

We list the key features of the proposed interval analysis procedure:

1. The procedure is applicable to closed loop systems whose characteristic function is continuous w.r.t. the uncertain parameters and is continuously differentiable (cf. also sec. 3.8) w.r.t. the amplitude and frequency variables of the periodic input signal to the nonlinear element. Subject to this assumption, the transfer function of the LTI element and the describing function of the nonlinear element can be described by any sequence of arithmetic expressions involving these variables and parameters, using $+$, $-$, $*$, $/$, $\sqrt{}$, \exp , \log , power, trigonometric functions, inverse trigonometric functions, etc. This means that the procedure is applicable to a very general class of nonrational LTI elements, nonlinear elements (including memoryless, memory, frequency independent, and frequency dependent types), and parametric uncertainty structures (including interval, affine, multilinear, and general nonlinear structures).
2. The procedure is guaranteed to find *all* limit cycle points within a given initial search region of amplitude and frequency ranges. Within the search region, the procedure computes rigorous guaranteed enclosures of all the limit cycle points to a *prescribed accuracy*. If no limit cycle points exist in the search region, the non-existence of the same is computationally verified.
3. The procedure is guaranteed to find all the limit cycle points in the search region, in a *finite* number of iterations. If there are no limit cycle points, the same is computationally rigorously verified in a finite number of iterations.
4. All limit cycle results generated by an interval arithmetic implementation of the procedure are *reliable*, that is, the results are trustworthy despite computational errors, such as round-off and truncation¹.

The rest of this paper is organized as follows. In section 2, we formulate the limit cycle computation problem as one of finding zeros of a parameter-dependent system of nonlinear equations. In section 3, we briefly describe the various IA tools that make up our procedure. We present the interval branch and bound procedure in section 4. In section 5, we demonstrate the procedure on two difficult examples.

¹However, any errors in the results of the limit cycle analysis due to the approximate nature of the DF method will remain.

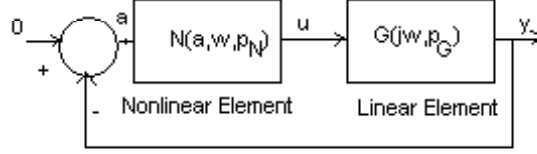


FIGURE 2.1. The closed loop nonlinear system.

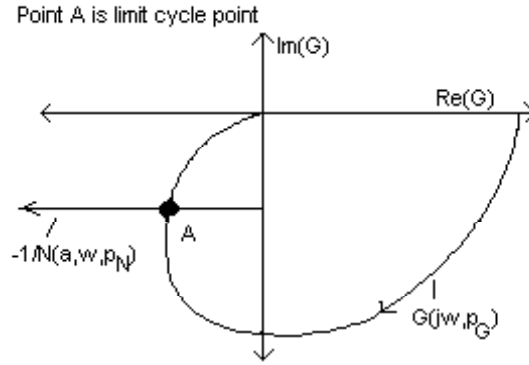


FIGURE 2.2. Graphical method of DF analysis.

2. THE ZERO-FINDING PROBLEM

Consider the closed loop system of Fig. 2.1, where $G(s, p_G)$ denotes the transfer function of the LTI element with parameter vector p_G , $\mathcal{N}(a, \omega, p_N)$ denotes the DF of the nonlinear element with parameter vector p_N , and a, ω denote the amplitude and frequency of the periodic input signal to nonlinear element. Under certain assumptions (see [3]), the necessary condition for existence of limit cycles is obtained from the characteristic equation of the nonlinear system in Fig. 2.1 as

$$(2.1) \quad 1 + \mathcal{N}(a, \omega, p_N) G(j\omega, p_G) = 0$$

When the DF does not depend upon ω , we can consider it as $\mathcal{N}(a, p_N)$, and find the limit cycle points *graphically* using (2.1) as the intersection(s) of the plots of $G(j\omega, p_G)$ and $\frac{-1}{\mathcal{N}(a, p_N)}$ in the complex plane, as shown in Fig. 2.2.

However, the graphical method is rather tedious and unsuitable when the nonlinearity is frequency dependent or when the LTI or nonlinear element has parameters with uncertain values. For such situations, we use a *computational* method to find the limit cycle points.

Expressing (2.1) in terms its real and imaginary components gives

$$(2.2) \quad f_{\text{Re}}(x, p) := \text{Re}\{1 + \mathcal{N}(a, \omega, p_N) G(j\omega, p_G)\} = 0; \quad f_{\text{Im}}(x, p) := \text{Im}\{1 + \mathcal{N}(a, \omega, p_N) G(j\omega, p_G)\} = 0$$

with

$$(2.3) \quad f(x, p) := (f_{\text{Re}}(x, p), f_{\text{Im}}(x, p)), \quad x := (a, \omega), \quad p := (p_G, p_N)$$

Then, from (2.1), (2.2), (2.3), limit cycles are predicted at all $x^* = (a^*, \omega^*)$ in the set

$$(2.4) \quad \mathcal{S}(f, \mathbf{x}^0, p) := \{x^* \in \mathbf{x}^0 : f(x^*, p) = 0\}$$

We refer to such a x^* as a limit cycle point in the search box \mathbf{x}^0 for p .

Next, suppose uncertainty exists in the parameters p_G and p_N of the LTI and nonlinear elements, with each parameter $p_i \in p$ varying independently over a given real interval $\mathbf{p}_i^0, i = 1, \dots, m$, where m denotes the total number of parameters (i.e., the length of the vector p). Then, we have a box $\mathbf{p}^0 = (\mathbf{p}_1^0, \dots, \mathbf{p}_m^0)$ of parameters, and the limit cycles for the uncertain nonlinear system are predicted at all x^* in the set

$$(2.5) \quad \mathcal{S}(f, \mathbf{x}^0, \mathbf{p}^0) := \{x^* \in \mathbf{x}^0 : \text{there exists some } p \in \mathbf{p}^0 \text{ such that } f(x^*, p) = 0\}$$

We refer to $x^* \in \mathcal{S}(f, \mathbf{x}^0, \mathbf{p}^0)$ as a limit cycle point in search box \mathbf{x}^0 for parameter box \mathbf{p}^0 . For brevity, we may sometimes simply refer to x^* as a limit cycle point in the box $(\mathbf{x}^0, \mathbf{p}^0)$.

From (2.5), we see that the problem of prediction of limit cycles is equivalent to the problem of finding all points x^* in the set \mathcal{S} . The latter is essentially the well-known problem of finding the zeros of a parameter-dependent system of nonlinear equations. We can (sometimes) find a solution to this problem using one of the following methods: (i) random search, (ii) an exhaustive grid search on the given box, (iii) more specialized or ad hoc methods such as the Jenkins-Traub method, and (iv) Homotopy continuation methods [17]. In contrast, IA methods provide rigorous enclosures of *all* solutions given by (2.5) to a prescribed accuracy. For a discussion of the various solution methods for solving parameter-dependent system of nonlinear equations, see [10].

3. INTERVAL ANALYSIS TOOLS

3.1. Initial search box. The amplitude a and frequency ω are nonnegative, so $x \in \mathbb{R}^{2+}$. However, instead of the semi-infinite box \mathbb{R}^{2+} for the search box \mathbf{x}^0 , in practice we use $[0, \text{real}_{\max}]^2$ where real_{\max} is the largest machine representable number on the computer. Further, some idea of the ranges in which limit cycle amplitudes and frequencies occur is often available in a particular problem. If so, the search box \mathbf{x}^0 can be limited to enclose these ranges. Alternatively, we can construct a ‘safe’ initial search box in which all limit cycle points are guaranteed to lie, using Moore’s procedure [16, chapter 6].

3.2. Natural interval extension. A natural interval extension of f can be simply obtained by replacing *real* variables and vectors with corresponding *interval* variables and vectors, and then evaluating f with interval arithmetic. We denote a natural interval extension of f on domain \mathbf{x} as $\mathbf{f}(\mathbf{x})$.

For instance, if $f(x) = 1 - 5x_1 + 1/3x_2^2 + 5$, then $\mathbf{f}(\mathbf{x}) = 1 - 5\mathbf{x}_1 + 1/3\mathbf{x}_2^2 + 5$ is the natural interval extension of f on \mathbf{x} . As another example, if $f(x) = x_1 \sin x_2 - x_3 \log x_2$, then $\mathbf{f}(\mathbf{x}) = \mathbf{x}_1 * \text{ISIN}(\mathbf{x}_2) - \mathbf{x}_3 * \text{ILOG}(\mathbf{x}_2)$ is the natural interval extension of f on \mathbf{x} , where *ISIN* and *ILOG* are the pre-declared interval sin and log functions in some programming language. A key property of natural interval extensions is the inclusion property.

Let $f^{\text{range}}(\mathbf{x})$ denote the range of f on \mathbf{x} . Then,

Theorem 3.1. [16] (*Inclusion property of natural interval extensions*):

$$f^{\text{range}}(\mathbf{x}) \subseteq \mathbf{f}(\mathbf{x})$$

3.3. Mean-value interval extension.

Lemma 3.2. [16] *Let $f : D \subseteq \mathbb{R}^n \rightarrow \mathbb{R}^n$ be a continuously differentiable function in the open domain D . Let \mathbf{f}' denote a natural interval extension of the Jacobian matrix f' on D . Then, for any box $\mathbf{x} \subseteq D$*

$$f(x) \in f(\hat{x}) + \mathbf{f}'(\mathbf{x})(x - \hat{x}) \quad \text{for all } x \in \mathbf{x}$$

where, \hat{x} is the midpoint of \mathbf{x} .

Proof. From the mean value theorem of calculus,

$$f(x) = f(\hat{x}) + f'(\zeta)(x - \hat{x}), \quad x \in \mathbf{x}$$

for some ζ between x and \hat{x} . Now $x, \hat{x} \in \mathbf{x} \Rightarrow \zeta \in \mathbf{x}$, so $f'(\zeta) \in f'^{\text{range}}(\mathbf{x})$. Applying the inclusion property of natural interval extensions (Theorem 3.1) to the Jacobian function f' gives $f'^{\text{range}}(\mathbf{x}) \subseteq f'(\mathbf{x})$. Hence the assertion of the lemma. ■

3.4. Zero exclusion test. Consider a search box $\mathbf{x} \subseteq \mathbf{x}^0$ and a parameter box $\mathbf{p} \subseteq \mathbf{p}^0$. To verify if \mathbf{x} contains any limit cycle points for \mathbf{p} , i.e., to verify existence of $x^* \in \mathcal{S}(f, \mathbf{x}, \mathbf{p})$, we can construct a natural interval evaluation \mathbf{f} for the function f in (2.3), and evaluate \mathbf{f} on the box (\mathbf{x}, \mathbf{p}) . By the inclusion property of natural interval extensions given in Theorem 3.1,

$$f^{\text{range}}(\mathbf{x}, \mathbf{p}) \subseteq \mathbf{f}(\mathbf{x}, \mathbf{p})$$

Hence,

$$\text{If } 0 \notin \mathbf{f}(\mathbf{x}, \mathbf{p}), \text{ then } 0 \notin f^{\text{range}}(\mathbf{x}, \mathbf{p})$$

Consequently, if $0 \notin \mathbf{f}(\mathbf{x}, \mathbf{p})$, then the limit cycle set $\mathcal{S}(f, \mathbf{x}, \mathbf{p})$ is empty, i.e., there are no limit cycle points in \mathbf{x} for \mathbf{p} , and the box (\mathbf{x}, \mathbf{p}) can be discarded.

However, due to interval dependency effects, $\mathbf{f}(\mathbf{x}, \mathbf{p})$ generally (considerably) overestimates the range $f^{\text{range}}(\mathbf{x}, \mathbf{p})$. Therefore, there may or may not be a limit cycle point in \mathbf{x} for \mathbf{p} , if $0 \in \mathbf{f}(\mathbf{x}, \mathbf{p})$. In this case, a more refined method, such as the generalized Krawczyk method, is needed. This method is next described.

3.5. The generalized Krawczyk method and fixed point theory. The Krawczyk method [13] is an enclosure method based on interval analysis for finding solutions of a system of nonlinear equations. The Krawczyk method considers the classical multivariate Newton method as a fixed point iteration. But whereas the classical Newton method only provides approximations to a zero, the Krawczyk method yields enclosures for the zero. Moreover, the classical Newton method provides no equivalent to the existence and non-existence tests possessed by the Krawczyk method.

The Krawczyk method is readily extended to the parameter-dependent case as follows. Suppose f in (2.3) is (Gateaux) differentiable with respect to x , and let f'_x denote the derivative of f with respect to x . Further, let \mathbf{f} and \mathbf{f}'_x denote the natural interval extensions of f and f'_x on the domain $(\mathbf{x}^0, \mathbf{p}^0)$. Let $\mathbf{x} \subseteq \mathbf{x}^0, \mathbf{p} \subseteq \mathbf{p}^0$ be nonempty search and parameter boxes. Let \hat{x} denote the midpoint of \mathbf{x} , and $Y \in \mathbb{R}^{2 \times 2}$ be an arbitrary nonsingular real matrix. Then, the generalized Krawczyk operator is defined as

$$(3.1) \quad \mathbf{K}(\mathbf{x}, \mathbf{p}) := \hat{x} - Y\mathbf{f}(\hat{x}, \mathbf{p}) + \{I - Y\mathbf{f}'_x(\mathbf{x}, \mathbf{p})\}(\mathbf{x} - \hat{x})$$

Further,

Theorem 3.3. [15] *(In above notation)*

1. *(Existence test for limit cycle points):*

If $\mathbf{K}(\mathbf{x}, \mathbf{p}) \subseteq \mathbf{x}$, then at least one limit cycle point exists in \mathbf{x} for every $p \in \mathbf{p}$

2. *(Non-existence test for limit cycle points):*

If $\mathbf{K}(\mathbf{x}, \mathbf{p}) \cap \mathbf{x} = \emptyset$, then there are no limit cycle points in \mathbf{x} (for any $p \in \mathbf{p}$)

Proof. The proof is largely based on properties of interval arithmetic and the Brouwer fixed point theorem. Consider a fixed but arbitrary $p \in \mathbf{p}$. Define the function g as

$$(3.2) \quad g(x, p) := x - Yf(x, p), \quad \text{for } x \in \mathbf{x}$$

Since f is continuous by hypothesis, g is also continuous. Further, the nonempty search box \mathbf{x} is clearly convex and compact. Then, by Brouwer's fixed point theorem [11],

$$g^{\text{range}}(\mathbf{x}, p) \subseteq \mathbf{x} \text{ implies the existence of some } x^* \in \mathbf{x} : g(x^*, p) = x^*$$

Moreover, as Y is nonsingular by hypothesis, this further implies $f(x^*, p) = 0$. That means, for nonsingular Y ,

$$(3.3) \quad g^{\text{range}}(\mathbf{x}, p) \subseteq \mathbf{x} \text{ implies the existence of a limit cycle point in } \mathbf{x}$$

By Lemma 3.2

$$f(x, p) \in f(\hat{x}, p) + \mathbf{f}'_x(\mathbf{x}, p)(\mathbf{x} - \hat{x}), \quad \text{for all } x \in \mathbf{x}$$

Substituting the above in (3.2) gives

$$\begin{aligned} g(x, p) &= x - Yf(x, p) \\ &\in x - Y\{f(\hat{x}, p) + \mathbf{f}'_x(\mathbf{x}, p)(\mathbf{x} - \hat{x})\} \\ &\in x - Yf(\hat{x}, p) - Y\mathbf{f}'_x(\mathbf{x}, p)(\mathbf{x} - \hat{x}), \quad \text{for all } x \in \mathbf{x} \end{aligned}$$

Therefore, by Theorem 3.1

$$\begin{aligned} g^{\text{range}}(\mathbf{x}, p) &\subseteq \mathbf{x} - Yf(\hat{x}, p) - Y\mathbf{f}'_x(\mathbf{x}, p)(\mathbf{x} - \hat{x}) \\ &\subseteq \hat{x} - Yf(\hat{x}, p) + \{I - Y\mathbf{f}'_x(\mathbf{x}, p)\}(\mathbf{x} - \hat{x}) \\ &\subseteq \mathbf{K}(\mathbf{x}, p) \end{aligned}$$

From (3.3) it follows that $\mathbf{K}(\mathbf{x}, p) \subseteq \mathbf{x}$ implies the existence of at least one limit cycle point in \mathbf{x} .

Further, if there is a point $x^* \in \mathbf{x}$ for which $f(x^*, p) = 0$, then from (3.2), $g(x^*, p) = x^*$. Hence, $x^* \in g^{\text{range}}(\mathbf{x}, p) \subseteq \mathbf{K}(\mathbf{x}, p)$. In other words, any limit cycle point in \mathbf{x} is also in $\mathbf{K}(\mathbf{x}, p)$. Therefore, if $\mathbf{K}(\mathbf{x}, p) \cap \mathbf{x} = \emptyset$ then there are no limit cycle points in \mathbf{x} .

The above arguments are for a fixed but arbitrary $p \in \mathbf{p}$. The assertions of the theorem for the (entire) parameter box \mathbf{p} follow readily by applying the arguments for every $p \in \mathbf{p}$. ■

Remark 3.1. (*exclusion tests*). If condition (2) in Theorem 3.3 is satisfied, then we discard (\mathbf{x}, \mathbf{p}) in our search for limit cycle points. We note that this exclusion test based on generalized Krawczyk operator is in addition to the zero exclusion test given in section 3.4.

Remark 3.2. From the above proof, it is evident that any limit cycle point in (\mathbf{x}, \mathbf{p}) is also in $\mathbf{K}(\mathbf{x}, \mathbf{p})$. So if $\mathbf{K}(\mathbf{x}, \mathbf{p}) \cap \mathbf{x} \neq \emptyset$, we can replace the box \mathbf{x} with the smaller box $\mathbf{x}' := \mathbf{K}(\mathbf{x}, \mathbf{p}) \cap \mathbf{x}$ and continue the search, without losing any limit cycle points that may be present in \mathbf{x} for \mathbf{p} .

Remark 3.3. (*The generalized Krawczyk method*) More precisely, if the enclosure of a limit cycle point is not tight enough (in terms of the side-lengths of \mathbf{x}), then by repeated application of the generalized Krawczyk operator, we can have an iterative method for improving the enclosures of limit cycle points. For a given \mathbf{p} , since $x^* \in \mathbf{x} \Rightarrow x^* \in \mathbf{K}(\mathbf{x}, \mathbf{p})$, it is natural to consider the iterations

$$(3.4) \quad \begin{aligned} \mathbf{x}^{(0)} &\leftarrow \mathbf{x} \\ \mathbf{x}^{(l+1)} &= \mathbf{K}(\mathbf{x}^{(l)}, \mathbf{p}) \cap \mathbf{x}^{(l)}, \quad l = 0, 1, 2, \dots \end{aligned}$$

Here we put $\mathbf{x}^{(l+1)} = \emptyset$ if $\mathbf{x}^{(l)} = \emptyset$. The method given by (3.4) is termed the generalized Krawczyk method.

3.6. Branching and bounding. If the initial search and parameter boxes are narrow enough, we can apply directly the generalized Krawczyk method. Then, the method starts with \mathbf{x}^0 in which we seek limit cycle points, and improves the enclosure of limit cycle points iteratively, till a prescribed accuracy (in terms of the side-lengths of \mathbf{x}) is achieved. As noted above, an important feature of this method is that it can be also used to computationally verify that there exists no limit cycle points in a search box.

Often, however, the initial search and parameter boxes are too wide, and bisection methods must complement the generalized Krawczyk method. The basic principle of a bisection method consists of repeated splitting of the search and parameter boxes (\mathbf{x}, \mathbf{p}) (this enables the ‘branching’ process) until they can be further reduced (this step involves ‘bounding’) by means of interval iteration. This branch and bound philosophy requires that a list of currently unprocessed boxes be stored in a list. Clearly, the method has no difficulties in also finding several

(isolated) limit cycle point regions in the initial search and parameter boxes $(\mathbf{x}^0, \mathbf{p}^0)$, since sooner or later such regions will be isolated by branching. For details of interval branching and bounding strategies, see [11].

3.7. Convergence and accuracy. Moore [16, Theorem 5.4] has shown that the condition $\mathbf{K}(\mathbf{x}, \mathbf{p}) \subseteq \text{interior of } \mathbf{x}$ is sufficient to guarantee the convergence of the method to all the zeros in \mathbf{x} . Further, using rounded interval arithmetic on a computing machine, the convergence to a prescribed accuracy can be obtained in a *finite* number of steps [16, sec 5.2, pp. 65-66]. Thus, we can compute arbitrarily tight enclosures of all possible limit cycle points in a given search region.

3.8. Non-differentiable functions and slope matrices. In the above, we assumed that f is Gateaux differentiable w.r.t. x . If it is not so, then a slope matrix of f may be used in place of the Jacobian. For details of slope matrices, see [11, sec 1.3]. Further, usage of slope matrices instead of Jacobians has an additional advantage that it leads to tighter enclosures of the limit cycle points.

4. A BRANCH AND BOUND PROCEDURE FOR LIMIT CYCLE COMPUTATIONS

In this section, we present an interval branch and bound procedure for constructing *enclosures* of *all* limit cycle points $x^* \in \mathcal{S}(f, \mathbf{x}^0, \mathbf{p}^0)$ to a *prescribed* accuracy. The proposed procedure uses the zero exclusion test and the generalized Krawczyk method in a branch and bound strategy to discard irrelevant parts of the initial search box \mathbf{x}^0 . Before giving the procedure, we define the class of closed loop systems and uncertainties to which the procedure can be applied.

Assumption 1. We assume that the function f is continuous w.r.t. p and continuously differentiable w.r.t. x on the box $(\mathbf{x}^0, \mathbf{p}^0)$. Subject to this assumption, the LTI transfer function G as well as the describing function \mathcal{N} can be described by any sequence of arithmetic expressions involving x and p using $+$, $-$, $*$, $/$, $\sqrt{}$, \exp , \log , power, trigonometric functions, inverse trigonometric functions, etc.

Remark 4.1. We require the continuity properties of f and its derivatives w.r.t. x , in order that the corresponding natural interval extensions also be continuous. The latter property ensures that the width of $\mathbf{f}(\mathbf{x})$ tends to zero as the width of \mathbf{x} tends to zero (by width of an interval, we mean the difference between the upper and lower endpoints of the interval), so that in turn, convergence and arbitrary accuracy can be achieved. If f is not differentiable w.r.t. x , then as mentioned in sec. 3.8, a slope matrix may be used in place of the derivatives.

Procedure to find enclosures of all limit cycle points in a given initial search region (cf. Remark 3.1) to a prescribed accuracy.

Inputs: the parameter box \mathbf{p}^0 , the search box \mathbf{x}^0 for limit cycle points, natural interval extensions \mathbf{f} and \mathbf{f}'_x , and an accuracy parameter ε for the limit cycle results.

Outputs: A list L^{sol} of boxes of maximum side lengths ε , such that all limit cycle points must lie in these boxes.

BEGIN Procedure

1. Set $\mathbf{x} \leftarrow \mathbf{x}^0$, $\mathbf{p} \leftarrow \mathbf{p}^0$ and initialize lists $L = \{\}$, $L^{sol} = \{\}$. Enter the box (\mathbf{x}, \mathbf{p}) into the list L .
2. (Start a fresh iteration): **Pop** all the boxes present in L for processing.
3. Discard irrelevant parts of all boxes:
 - (Find Natural interval evaluations): Evaluate \mathbf{f} over all the boxes (\mathbf{x}, \mathbf{p}) .
 - (Perform zero exclusion test): Discard all those boxes (\mathbf{x}, \mathbf{p}) for which $0 \notin \mathbf{f}(\mathbf{x}, \mathbf{p})$. If there are no more boxes remaining, go to step 7.
 - (Find derivatives and setup Krawczyk operator): Evaluate \mathbf{f}'_x , and set up the generalized Krawczyk operator as defined in (3.1) for all boxes (\mathbf{x}, \mathbf{p}) .
 - (Perform generalized Krawczyk test): Find and discard all boxes (\mathbf{x}, \mathbf{p}) for which condition (2) in Theorem 3.3 is satisfied. If there are no more boxes remaining, go to step 7. Else, obtain smaller boxes $(\mathbf{x}', \mathbf{p})$ containing the limit cycle points from the remaining boxes (\mathbf{x}, \mathbf{p}) , where $\mathbf{x}' = \mathbf{K}(\mathbf{x}, \mathbf{p}) \cap \mathbf{x}$.

4. (Extract Solutions): Find all boxes (\mathbf{x}, \mathbf{p}) for which \mathbf{x} have side-lengths at most equal to ε , and deposit the corresponding \mathbf{x} in L^{sol} . Then, discard all such boxes (\mathbf{x}, \mathbf{p}) from processing.
5. (Perform Tessellation): If there are no boxes remaining, go to step 7. Else, for each remaining box (\mathbf{x}, \mathbf{p}) , find the coordinate direction along which it is longest, and bisect it along this direction. Push all the resulting halved boxes into the list L .
6. (Terminate current iteration): Go to step 2.
7. Stop.

END procedure.

Remark 4.2. *An interval arithmetic implementation of proposed procedure gives reliable results, i.e., the results are trustworthy despite computational errors, see [12].*

5. ILLUSTRATIVE EXAMPLES

We programmed the proposed procedure using the interval arithmetic toolbox INTLAB [20] on a PC/Pentium-III 850 MHz machine with 256 MB RAM. We extensively tested the procedure on several nonlinear system examples given in [9], [6],[21], [19], [8], [3],[7]. These examples cover

1. LTI elements of different types
 - (a) Rational elements
 - (b) Nonrational elements
2. Different parametric uncertainty structures
 - (i) independent
 - (ii) affine linear
 - (iii) multilinear
 - (iv) nonlinear
3. Nonlinear elements of different types
 - (a) Frequency independent nonlinearities
 - (i) memoryless: ideal relay, saturation, deadzone
 - (ii) memory type: backlash, relay with hysteresis, relay with deadzone and hysteresis
 - (b) Frequency dependent nonlinearities
 - (i) Clegg integrator

Here, space considerations permit us to discuss only two examples. We select these two examples in order to demonstrate the wide range of applicability of the proposed procedure.

Note: for convenience, in this section we use the notation $G(s)$ and \mathcal{N} , for $G(s, p_G)$ and $\mathcal{N}(a, \omega, p_N)$, respectively.

Example 5.1: The first example demonstrates the applicability of the proposed procedure to nonrational transfer functions, general nonlinear parametric dependency structures, and nonlinearities of memory type. The LTI element is a third order nonrational transfer function having nonlinear parametric dependency

$$G(s) = \frac{(1 + \sqrt{\lambda_1 \lambda_3}) \cdot s \cdot e^{-\lambda_2 \cdot \lambda_3 \cdot s}}{\ln(\lambda_3) \cdot s^2 + \cos(\frac{\lambda_3}{2.5} + \lambda_1 \lambda_2) \cdot s + 1}, \quad \lambda_1 \in [0.1, 0.2], \lambda_2 \in [0.2, 0.3], \lambda_3 \in [13, 17]$$

The nonlinear element is of memory type, in the form of a hysteresis element having relay output $M = \pm 1$ and uncertainty in the total hysteresis as $H \in [0.3, 0.4]$. We choose the initial search box for limit cycle points as $\mathbf{x} = ((0.4, 100], [0.01, 100])$, and set the prescribed accuracy $\varepsilon = 0.1$.

Proposed procedure: We execute the proposed procedure, and obtain a set of 14,997 boxes enclosing the limit cycle points. The procedure takes 26 iterations and 455 seconds to generate these limit cycle enclosures. The results are plotted in Fig. 5.1.

TABLE 5.1. Comparison of limit cycle results obtained using proposed, graphical, and simulation methods in Example 5.1

Case	Variable	Proposed Procedure	Graphical	Simulation	Property
Case 1	Amplitude-1	[4.5041, 4.5042]	4.5041	4.58	Stable
	Frequency-1	[0.6679, 0.6680]	0.6680	0.668	
Case 2	Amplitude-1	[2.9455, 2.9456]	2.9455	2.82	Stable
	Frequency-1	[0.5973, 0.5974]	0.60	0.59	
	Amplitude-2	[0.4522, 0.4527]	0.452	—	Unstable
	Frequency-2	[1.8228, 1.8233]	1.82	—	
Case 3	Amplitude-1	[3.6144, 3.6264]	3.6144	3.514	Stable
	Frequency-1	[0.5260, 0.5266]	0.5263	0.527	
	Amplitude-2	[0.7447, 0.7454]	0.7450	—	Unstable
	Frequency-2	[1.4057, 1.4060]	1.4058	—	

We next cross-check these results versus those of the graphical method and nonlinear simulations. To enable cross-checking, we pick (arbitrarily) a few combinations of parameter values from the given parameter ranges, and designate them as various cases as follows.

Case 1: $\lambda_1 = 0.1, \lambda_2 = 0.2, \lambda_3 = 13, H = 0.3$

Case 2: $\lambda_1 = 0.15, \lambda_2 = 0.25, \lambda_3 = 15, H = 0.35$

Case 3: $\lambda_1 = 0.2, \lambda_2 = 0.3, \lambda_3 = 17, H = 0.4$

The limit cycle points (amplitude and frequency) obtained using the proposed procedure are given in column 3 of Table 5.1 for the various cases.

Graphical method: Fig. 5.2 shows the polar plots of $G(j\omega)$ and $-1/N$ for the three cases. As mentioned in section 2, we can find the limit cycle points graphically as the intersections of the plots of $G(j\omega)$ and $-1/N$; for this task, we use the enlarged plot in Fig. 5.3. The limit cycle points obtained with the graphical procedure are given in column 4 of Table 5.1 for the various cases. In all cases, we find the results of the proposed procedure to be nearly identical to those of the graphical method.

Nonlinear simulations: The closed loop (as in Fig. 2.1) nonlinear simulations are performed using the SIMULINK toolbox of MATLAB [1]. The simulation results are plotted in Fig. 5.4 for the various cases. From the figure, we record the limit cycle amplitudes and frequencies, and report them in column 5 of Table 5.1. The Table shows minor differences between the results of nonlinear simulations and the proposed procedure. However, such minor differences are perhaps expected, due to the approximate nature of the DF method itself.

Example 5.2: This example demonstrates further the applicability of the proposed procedure to include frequency dependent nonlinearities. The LTI element is a second order transfer function

$$G(s) = \frac{\lambda_0}{\lambda_1 s^2 + \lambda_2 s + \lambda_3}, \quad \lambda_0 \in [10, 20], \lambda_1 \in [1, 2], \lambda_2 \in [1, 2], \lambda_3 \in [1, 2]$$

and the nonlinear element is a Clegg integrator having a frequency dependent describing function

$$\mathcal{N} = \frac{4}{\pi\omega} \left(1 - j\frac{\pi}{4}\right)$$

The Clegg integrator is a nonlinear integrator that can be used as a more efficient compensator than a LTI integrator, see [7, pp 79 - 81]. We note that the DF of a Clegg integrator is dependent on the frequency but not on the amplitude of the input signal. We therefore choose the initial search box for limit cycle points as $\mathbf{x} = ([1, 1], [0.01, 100])$, and set the prescribed accuracy $\varepsilon = 0.025$.

We execute the proposed procedure, and obtain a set of 3060 boxes enclosing the limit cycle points. The procedure takes 31 iterations and 6 seconds to generate these limit cycle enclosures. The procedure outputs a

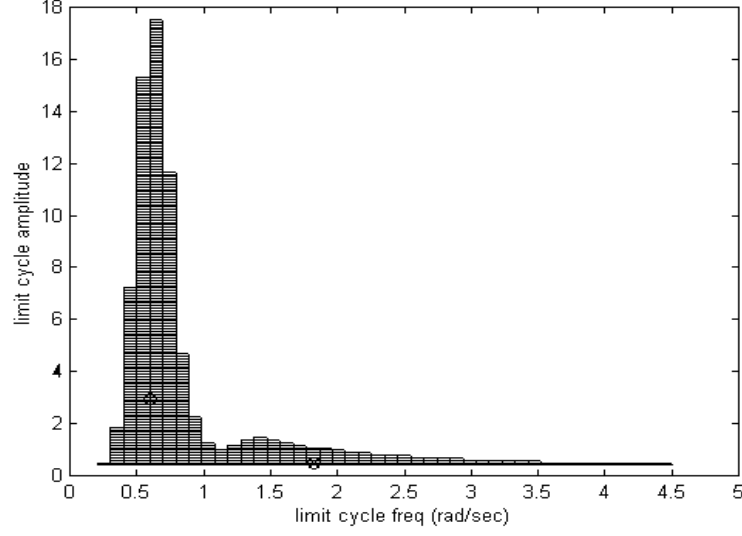


FIGURE 5.1. Limit cycle enclosures obtained using proposed procedure in Example 5.1.

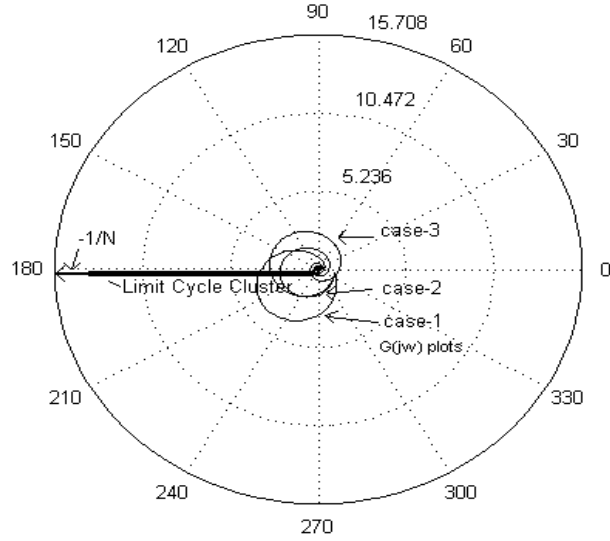


FIGURE 5.2. Polar plot of $G(j\omega)$ and $-1/N$ for the three cases in Example 5.1. This plot is used to graphically obtain the limit cycle points for the three cases to cross-check the results of the proposed procedure.

limit cycle cluster with frequencies in the interval $[2.3535, 3.1836]$. The amplitude of the limit cycle is immaterial in this example, as the DF of the Clegg integrator is amplitude independent.

As in the earlier example, to enable cross-checking of our results, we pick (arbitrarily) a few combinations of parameter values from the given parameter ranges, and designate them as various cases as follows.

Case 1: $\lambda_0 = 10, \lambda_1 = 1, \lambda_2 = 1, \lambda_3 = 1$

Case 2: $\lambda_0 = 20, \lambda_1 = 2, \lambda_2 = 2, \lambda_3 = 2$

For these two cases, the proposed procedure gives an empty L^{sol} list, that is, it predicts that no limit cycles exist. We next proceed to cross-check this finding using graphical and simulation methods.

Graphical method: Fig. 5.5 shows the polar plots of $G(j\omega)$ and $-1/N$, for case 1. We see that in this figure, although the plots of $G(j\omega)$ and $-1/N$ intersect, the frequencies at the point of intersection are different.

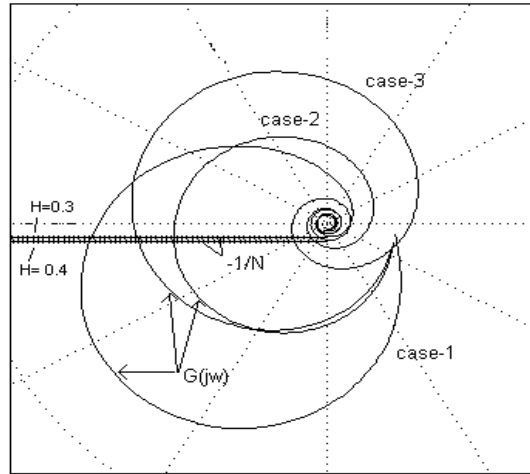


FIGURE 5.3. The previous polar plot is zoomed here to show more clearly the limit cycle points for the three cases in Example 5.1.

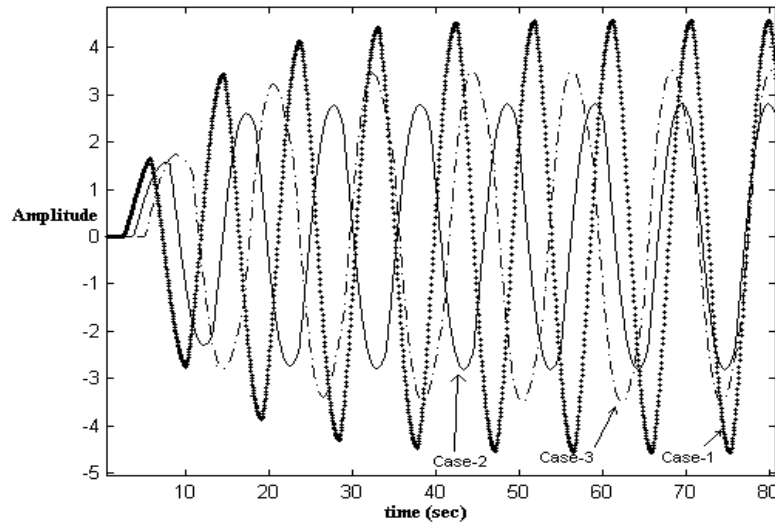


FIGURE 5.4. Closed loop nonlinear simulation results for the three cases in Example 5.1. Case-1 (dotted), case-2 (solid), and case-3 (dashed) lines.

These frequencies are $\omega = 1.82$ for $G(j\omega)$, and $\omega = 5.47$ for $-1/N$. Hence, the graphical method confirms the non-existence of limit cycles for case 1. For case 2, at the point of intersection, we find that the frequencies are $\omega = 3.45$ for $G(j\omega)$, and 2.88 for $-1/N$. Hence, the graphical method confirms the non-existence of limit cycles also for case 2.

Nonlinear simulations: The closed loop simulation responses obtained with SIMULINK do not exhibit any limit cycle behavior for these two cases. This further confirms the findings of the proposed procedure for the two selected cases.

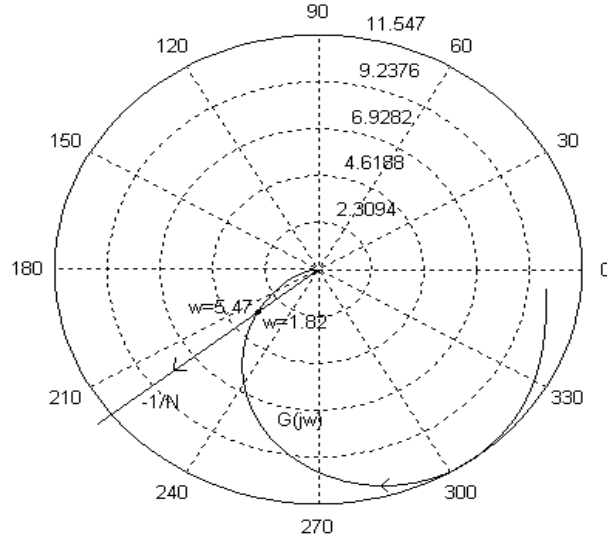


FIGURE 5.5. Polar plot of $G(j\omega)$ and DF curve $-1/N$ for case 1 in Example 5.2. Though these plots intersect, the frequencies at the intersection point are different. Thus, no limit cycle points are predicted for this case.

6. CONCLUSIONS

We have presented a branch and bound procedure for limit cycle analysis of nonlinear systems in the presence of parametric uncertainties in the LTI and nonlinear elements. The procedure has a wide scope of applicability that covers nonrational LTI elements, nonlinear elements (involving memoryless, memory, frequency independent, or frequency dependent type), and parametric uncertainty structures (including interval, affine, multilinear, or general nonlinear structure). The procedure computes rigorous guaranteed enclosures of all the limit cycle points to a prescribed accuracy. If no limit cycle points exist in the initial search region, the non-existence of the same is computationally verified. We have extensively tested the procedure on several examples, and successfully validated the results with those of graphical and simulation methods.

REFERENCES

- [1] *MATLAB user guide, version 5.3*. The MathWorks Inc., MA, USA, 2000.
- [2] T. C. Anthony, B. Wie, and S. Carroll. Pulse modulated control synthesis of a flexible spacecraft. *Journal of Guidance*, 13(6):1014–1022, 1990.
- [3] D. P. Atherton. *Nonlinear control Engineering*. Van Nostrand, 1975.
- [4] C.H. Chang and M.K. Chang. Analysis of gain margins and phase margins of a nonlinear reactor control system. *IEEE Transactions on Nuclear Science*, 41(4):1686–1691, 1994.
- [5] M. S. Fadali and N. chachavalvoong. Describing function analysis of uncertain nonlinear systems using the Kharitonov approach. In *Proc. of ACC*, pages 2908–2912, Seattle, 1995.
- [6] G. Ferreres and V. Fromion. Nonlinear analysis in the presence of parametric uncertainties. *International Journal of Control*, 69, 1998.
- [7] A. Gelb and W. E. Vander Velde. *Multiple-Input Describing Functions and Nonlinear System Design*. McGraw-Hill, 1968.
- [8] I.J.Nagarath and M. Gopal. *Control system engineering*. Wiley Eastern, New Delhi, 1995.
- [9] S. T. Impram and N. Munro. Describing function analysis of nonlinear systems with parametric uncertainties. In *Proceedings of UKACC Int. conf. on CONTROL 98*, 1998.
- [10] R. B. Kearfott. Some tests of generalized bisection. *ACM Transactions on Mathematical Software*, 13(3):197–220, 1987.
- [11] R. B. Kearfott. *Rigorous global search: continuous problems*. Dodrecht: Kluwer Academic Publishers, 1996.
- [12] R. Klatte, U. Kulisch, M. Neaga, D. Ratz, and Ch. Ullrich. *PASCAL-XSC language reference with examples*. Springer-Verlag, Berlin Hidelberg, 1993.
- [13] R. Krawczyk. Newton algorithmen zur bestimmung von nullstellen mit fehler-schranken. *Computing*, 4:187–201, 1969.
- [14] R. E. Moore. *Interval analysis*. Prentice-Hall, Englewood Cliffs, New Jersey, 1966.

- [15] R. E. Moore. A test for existence of solutions to nonlinear systems. *SIAM J. Numerical Analysis*, 14(4):611–615, 1977.
- [16] R. E. Moore. *Methods and applications of interval analysis*. SIAM, Philadelphia, 1979.
- [17] A. P. Morgan. *Solving polynomial systems using continuation for engineering and scientific problems*. Prentice-Hall, Englewood Cliffs, N. J., 1987.
- [18] B. Newman. Dynamics and control of limit cycling motions in boosting rockets. *Journal of Guidance Control and Dynamics*, 8(2):280–286, 1995.
- [19] K. Ogata. *Modern control engineering*. Prentice Hall of India, New Delhi, 1997.
- [20] S. M. Rump. INTLAB - interval laboratory. In T. Csendes, editor, *Developments in reliable computing*. Kluwer Academic Publishers, 1999.
- [21] J. E. Tierno. Describing function analysis in the presence of uncertainty. *Journal of Guidance, Control and Dynamics*, 20, 1997.